

Article Info

Received: 23 Apr 2021 | Revised Submission: 28 Jul 2021 | Accepted: 05 Sept 2021 | Available online: 15 Sept 2021

Experimental and Numerical Studies of Electrolyte Concentration Effect in Electrochemical Discharge Based Micro-drilling

Viveksheel Rajput*, Mudimallana Goud** and Narendra Mohan Suri***

ABSTRACT

Electrochemical discharge based micro-drilling (ECDD) is a hybrid machining process that involves the thermal heating of the sparks and etching action of the electrolyte for material removal mechanism. The concentration of the electrolyte plays a vital role in determining the material removal rate (MRR) during the micro-hole drilling process since a higher depth is desired. Despite numerous experimental studies, the reporting of numerical studies concerning the effect of electrolyte concentration on MRR is still scarce. The present article focuses on the development of a finite element based thermal model for studying the MRR of glass material concerning electrolyte concentration. The model is validated using previously reported as well as present experimental studies. MRR is observed to be in fair agreement with the experimental MRR. Results revealed that the MRR improves with the increase in electrolyte concentration due to the increase in the imported heat flux over the work material. MRR improvement is the combined result of an increase in thermal energy as well as an increase in hydroxide (OH) ions that further enhances the chemical etching action. The present study successfully demonstrates the application of numerical aspects for analyzing the MRR in the ECDD process concerning electrolyte concentration.

Keywords: Finite Element Modeling; Spark Radius; Material Removal Rate; Concentration; Glass.

1.0 Introduction

Electrochemical discharge drilling (ECDD) is known for machining non-conductive materials like quartz, ceramics and glass etc. The material removal mechanism is the combined effect of electric discharge machining (EDM) and electrochemical machining (ECM). It was first reported by the Kurafuji and Suda in 1968 [1] in which they described the possibility of drilling the glass using electrical discharge. Basak and Ghosh [2] elaborated the spark mechanism in ECDD process and highlighted the critical voltage-current values for generating the spark. The process consists of two electrodes (cathode and anode), both dipped in an aqueous solution of electrolyte alongside work material as shown in Figure 1. The application of power supply prompts the formation of tiny hydrogen and oxygen bubbles at the cathode and anode respectively. The tiny hydrogen bubbles combine physically with each other to form the gas

film at the surrounding area of the tool electrode (cathode). It hinders the flow of electrons in the circuit; and as a result, high amount of electric field is generated in the film. Thereafter, the spark is occurred through the tool electrode owing to electric breakdown of the gas film. Thereafter, the material is removed due to the thermal heating of the sparks followed by the chemical etching movement [3-4]. Rajput et al. [5-6] successfully demonstrate the applications of ECDD process for fabricating micro-holes on glass and silica material. It was observed that MRR and hole depth increases with the increase in electrolyte concentration. Wuthrich et al. [7-8] made distinct contribution in the field of ECDD covering various parameters such as tool feed, electrolyte concentration, deep drilling etc.

2.0 Numerical Studies

Various numerical studies have been reported for analyzing the ECDD process. Jain et al.

*Corresponding author; Department of Mechanical Engineering, Punjab Engineering College, Chandigarh, India (E-mail: sheelrajput03@gmail.com)

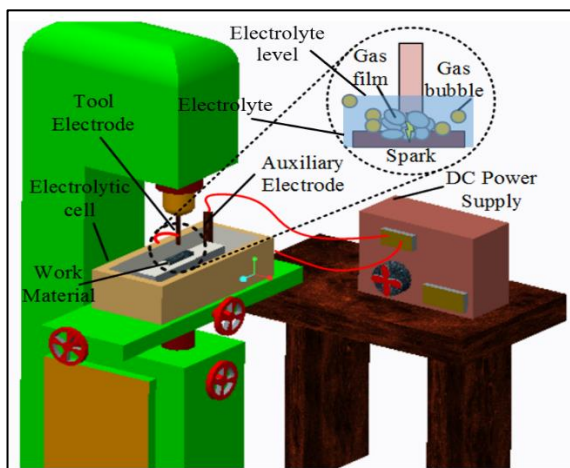
, *Department of Mechanical Engineering, Punjab Engineering College, Chandigarh, India

[9] studied the process based on finite element simulation and assumed sparks to be successive in nature. They utilized the application of uniform gaussian heat within the spark region. Bhondwe et al. [10] built a 2D FEM based thermal model for analyzing the MRR and assumed Gaussian heat application within the spark region. The predicted results are in fair agreement with the experimental results. Wei et al. [11] also built a FEM based transient thermal model to simulate a single spark for discharge. Goud et al. [12] successfully developed a 3D FEM model for predicting MRR at different electrolyte concentration. The predicted results are in acceptable range when compared to previously report experimental studies.

Rajput et al. [13-15] also built a FEM based thermal model for comparing the different work materials and electrolytes using Gaussian heat input. NaOH and KOH are the preferred electrolytes since they produce more MRR compared to other electrolytes such as NaCl, KCl etc. the application of Gaussian heat input represents a true nature of the heat in which heat is maximum at the spark center and decreases with the increase in radial distance. Based on literature, it is concluded that despite having numerical studies in this process, need is still there to study the numerical aspects of this process. This article focusses on the development of the thermal model for analyzing the MRR with respect to the change in electrolyte concentration. The developed model is validated using previously reported as well as present experimental studies.

3.0 Model Methodology

Fig. 1: ECDD Schematic Diagram [5]



A finite element based thermal model is developed to estimate the MRR of glass work material concerning different electrolyte concentrations. Work material of dimensions 0.3 X 0.3 X 0.4 mm³ is chosen as a domain for developing and applying boundary conditions as shown in Figure 2. The key properties of the soda lime glass used in numerical study is given in Table 1.

Fig. 2: FEM Thermal Model with Boundary Conditions [13]

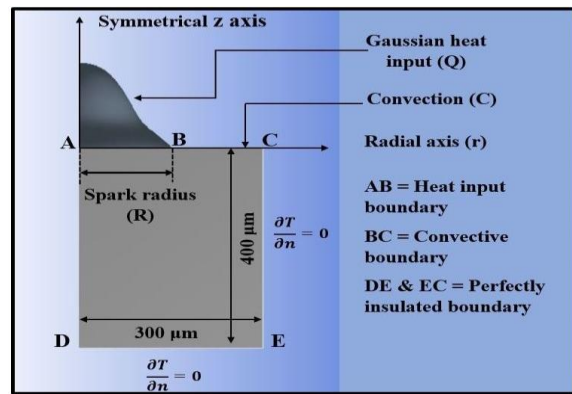


Table 1: Glass Properties Used in Numerical Study [10,12]

Property	Soda-lime glass
Thermal Conductivity (W/mK)	1.6
Heat Capacity (J/kg-K)	670
Melting temperature (K)	1673
Room temperature (K)	295
Density (Kg/m3)	2100
Convective coefficient (W/m2-K)	10000

3.1 Assumptions

The following assumptions are utilized during the numerical study of ECDD process.

- Work material properties are assumed homogeneous in nature.
- Only one spark under the tool tip in a single time with a duration of 150 μs is assumed [10,12].
- The distribution of the heat is assumed Gaussian.
- The shape of the cavity or crater formed is assumed hemispherical or dome shaped.
- The transference of the heat energy to the work material (E_p) is selected as $E_p = 20\%$ [3].
- Machining conditions during the ECDD process remains constant.
- Spark radius of 150 μm is used in this study [10].

3.2. Boundary conditions

The work material temperature is assumed to be at room temperature (T_0) at an initial time i.e., $t=0$. Boundary AB is the heat input boundary on the top surface of the work material and obtains a gaussian heat input (H) as illustrate in equation 1 (Figure 2).

$$H = \frac{4.45E_pVI}{Area\ of\ Spark} \exp \left\{ -4.5 \left\{ \left(\frac{r_x}{R} \right)^2 + \left(\frac{r_y}{R} \right)^2 \right\} \right\} \dots(1)$$

Where, E_p is the energy transference, V and I are the critical current and voltage values, r is the radial distance and R is the spark radius. The effect of heat input on the other boundaries (DE & CE) is assumed negligible and observe to be perfectly insulated. No heat transfer occurs across these boundaries. For boundary AD, the generation of the heat is symmetrical.

$$\frac{\partial T}{\partial n} = 0, t \geq 0 \dots(2)$$

The remaining top boundary over the top work material is the convective boundary i.e., BC and it releases heat to the atmosphere; expressed as $C = h(T - T_0)$... (3)

Where, h is a convective coefficient, T is work material temperature, T_0 is room temperature.

3.3. Role of electrolyte concentration (C)

Electrolyte concentration plays a significant role in determining the MRR since it controls the amount of current passage through the circuit. The current (I) in Eq (2) is a function of electrolyte concentration and computed using Eq (4) as given below for NaOH electrolyte [10]. With the increase in electrolyte concentration, there is an increase in the current values that further improves the total heat input over the work material.

$$I = 3.2323 \times 10^{-5} C^3 - 0.0027056 C^2 + 0.091378 C + 0.71429 \text{ (NaOH)} \dots(4)$$

3.4 Analytical estimation of MRR

The MRR of glass is estimated by using the temperature plots of isothermal curves obtained in simulation as shown in Figure 3. The material removal in ECDD is directly proportional to the increase in work material temperature. Therefore, the MRR is assumed to be removed when work material temperature (T) becomes larger than the work material melting temperature (T_m). It is expressed as $T > T_m$... (5)

The criteria for material removal due to a single spark is shown in Figure 4. The volume removed due to single spark at the melting temperature is calculated using r_m and z_m intercepts, given as-

$$V_m = \iiint r_m z_m \theta \ drdzd\theta = \frac{2}{3} \pi r_m^2 z_m \dots(6)$$

The volume of the material removed per unit time, is given

$$V_T = V_m \times (\text{number of sparks per unit time}) \dots(7)$$

The final MRR is computed as

$$MRR = V_T \times (\text{Work material density } (\rho)) \dots (8)$$

Fig. 3: Temperature Distributions at 15 wt.% and 40 V

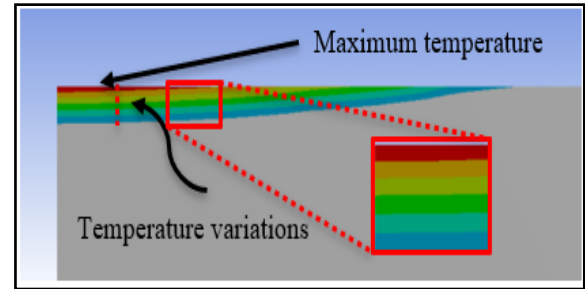
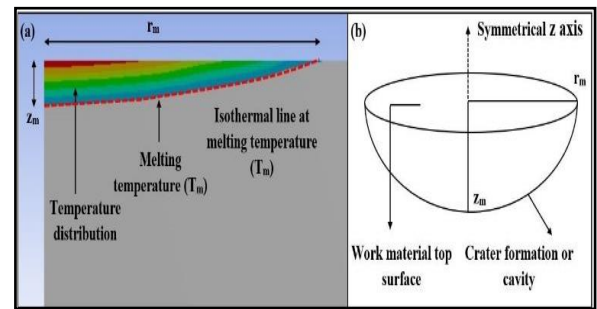


Fig. 4: Criteria of MRR Estimation [13]

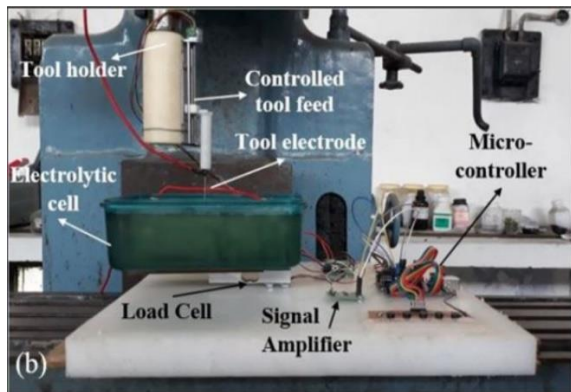


4.0 Experimental Details

The experiments are carried out to validate the predicted MRR at different electrolyte concentrations for the glass work material. The experiments are performed on the developed adaptive tool feed based experimental setup which is attached to vertical milling machine (Make: Fridge Werner Type-FV-1) as shown in Figure 4. The adaptive tool feed method helps in maintaining the constant machining gap and prevents the tool contact with the work material. It uses the sensitive load cell

that senses the physical contact between the tool and the work material. As soon as the physical contact is detected, the load cell produces a potential difference that further sends a signal to micro-controller. It reverses the motor direction and retracts the tool in order to prevent the contact. Table 2 presents the machining conditions used during experimental studies.

Fig. 5: Adaptive Tool Based Experimental Setup [14]



4.1 Experimental MRR

MRR is computed as the weight difference of the glass material before and after micro-hole fabrication during ECDD process divided by the total time (t) [5].

Table 2: Machining Conditions Used in Experimental Study

Parameter	Value
Applied Voltage	45 V
Electrolyte	NaOH
Electrolyte Concentration	15 wt.% - 45 wt.%
Tool Feed Rate	3 mm/min
Tool Immersion depth	1mm (Approx.)
Tool Material	Stainless steel
Tool Shape	Cylindrical
Tool Size	1 mm
Inter Electrode Gap	35 mm
Machining time	2 min

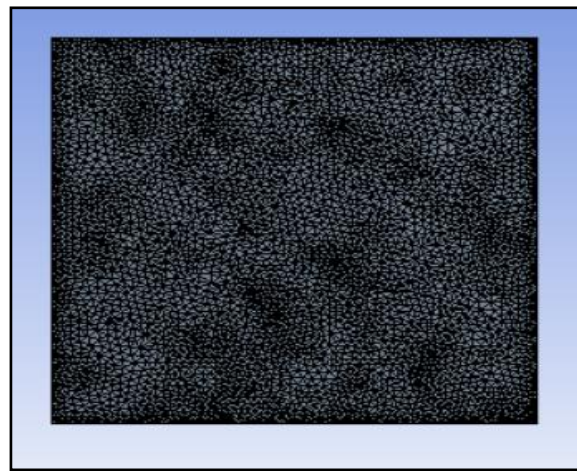
5.0 Results and Discussions

5.1 Model validations

A FEM based thermal model is developed to study the ECDD process numerically using the distribution plots of temperature as shown in Figure

3. The developed model is meshed with the tetrahedron mesh methods before moving to the solver. It is done to improve the accuracy in the simulation results. The meshed model is shown in Figure 6. The developed model is validated by comparing the work material temperature obtained in a radial direction with previously reported model given by Goud et al. [12] as shown in Figure 7.

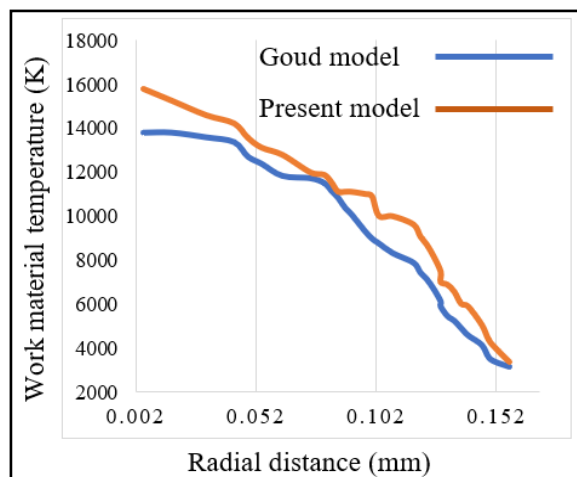
Fig. 6: Meshed Model



It is observed that the variation of the temperature is similar that dictates the model validation. However, few differences in the temperature values are also seen that may be accounted by the fact that the application of Gaussian heat input is different in both the models.

5.2. MRR validations

Fig. 7: Work material temperature comparison



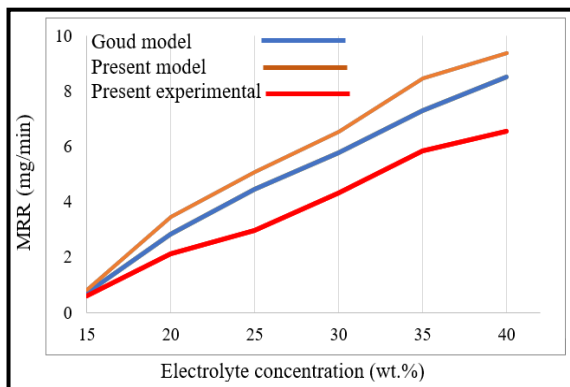
Moreover, the model is further assessed and validated by comparing the predicted MRR with the previously reported simulations and present experimental results at different NaOH concentrations as shown in Figure 8.

The trend of MRR variation is similar and found to be in acceptable range when compared to previous studies. A reasonable agreement is found between the experimental and predicted MRR. A maximum difference of 2.8 mg/min in MRR is seen at 40 wt.% because of the different assumptions made in the numerical study of ECDD process such as spark radius, energy transference, etc.

5.3 Effect of electrolyte concentration on predicted MRR

Figure 8, illustrates the plot of predicted MRR at different NaOH concentrations. An improvement of 8.5 mg/min in the predicted MRR is observed with the increase in electrolyte concentration from 15 wt.% to 40 wt.%. Since current (I) is a function of electrolyte concentration, any increase in concentration improves the heat input. Therefore, any increase in electrolyte concentration leads to an improvement in the imported heat flux that is applied on the top surface of the work material. As a result, an increase in work material temperature is seen with the increase in concentration. Figure 9 shows the simulation results of work material temperature obtained at 15 wt.% and 40 wt.%. An increase of 155.8 K in work material is observed with the increase in concentration.

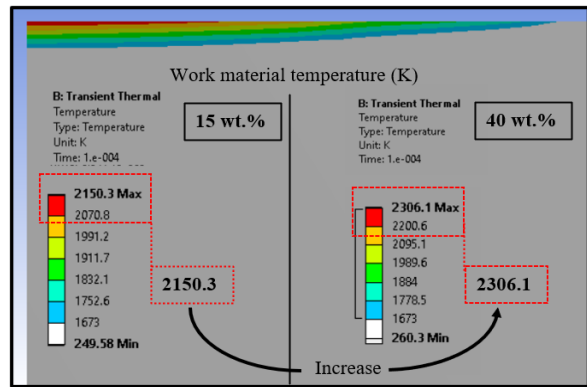
Fig. 8: Comparison of MRR Variation



Experimentally it is observed that any change in electrolyte concentration leads to change in

ion mobility that further alters its conductivity. The formation rate of hydrogen bubbles increases at a higher conductivity which further accelerates the gas film formation. Hence, high frequency of sparks happens over the work material. Hence, higher MRR is acquired.

Fig. 9: Work Material Temperature Comparison at 15 wt.% and 40 wt.%



6.0 Conclusions

In this present investigation, FEM based thermal model is developed to analyse the MRR at different electrolyte concentrations. The model is validated and assessed by comparing the predicted MRR with previously reported simulated studies as well as experimental studies. The effect of electrolyte concentration on predicted MRR is also seen. The major conclusions drawn from the present study are given below:

- The present developed model exhibits fair agreement with the experimental MRR when compared to predict MRR during ECDD process.
- The Gaussian distribution of heat represents the true nature of heat existing within the spark region.
- The predicted MRR improves with the increase in electrolyte concentration, since any increase in concentration enhances the imported heat flux over the top surface of work material. An increase in thermal energy is observed with the increase in electrolyte concentration.
- An increase of 155.8 K in work material temperature and 8.5 mg/min in MRR is observed with the increase in electrolyte concentration from 15wt.% to 40wt.%.

7.0 Acknowledgment

Authors acknowledge the support provided by the Punjab Engineering College, Chandigarh, India.

References

- [1] H Kurafuji, K Suda. Electrical discharge drilling of glass. *Ann. CIRP* 16, 1968, 415–419.
- [2] I Basak, A Ghosh. Mechanism of material removal in electrochemical discharge machining a theoretical model and experimental verification. *J Mater Process Tech* 71, 1997, 350-359. DOI:10.1016/S0924-0136(97)00097-6
- [3] A Kulkarni, R Sharan, GK Lal. An experimental study of discharge mechanism in electrochemical discharge machining. *Int J Mach Tool Manuf* 42, 2002, 1121–1127.
- [4] B Bhattacharyya, BN Doloi, SK Sorkhel. Experimental investigations into electrochemical discharge machining (ECDM) of non-conductive ceramic materials. *Journal of Materials Processing Technology*, 95, 1999, 145-154.
- [5] V Rajput, SS Pundir, MM Goud, NM Suri. Multi-Response Optimization of ECDM Parameters for Silica (Quartz) Using Grey Relational Analysis. *Silicon*, 2020. DOI: 10.1007/s12633-020-00538-7
- [6] V Rajput, MM Goud, NM Suri. Performance Analysis of ECDM Process Using Surfactant Mixed Electrolyte 2020.
- [7] V Sharma, U Dixit, K Sørby, A Bhardwaj, R Trehan. *Manufacturing Engineering. Lecture Notes on Multidisciplinary Industrial Engineering*.
- [8] V Fascio, R Wuthrich, H Bleuler. Spark assisted chemical engraving in the light of electrochemistry. *Electrochim Acta*. 49, 2004, 3997–4003.
- [9] R Wuthrich, LA Hof, A Lal. Physical principles and miniaturization of spark assisted chemical engraving (SACE). *J Micromech Microeng*. 15, 2005, 102005. DOI: 10.1088/0960-1317/15/10/S03
- [10] VK Jain, PM Dixit, PM Pandey. On the analysis of the electrochemical spark machining process. *Int J Mach Tools Manuf*. 39, 1999, 165–186.
- [11] KL Bhondwe, V Yadava, G Kathiresan. Finite element prediction of material removal rate due to electrochemical spark machining. *Int J Mach Tools Manuf* 46, 1699–1706. DOI: 10.1016/j.ijmachtools.2005.12.005
- [12] C Wei, K Xu, J Ni. A finite element-based model for electrochemical discharge machining in discharge regime. *Int J Adv Manuf Technol*. 54, 2011, 987–995.
- [13] MM Goud, AK Sharma. A three-dimensional finite element simulation approach to analyze material removal in electrochemical discharge machining. *Proceedings of the Institution of Mechanical Engineers, Part C: Journal of Mechanical Engineering Science*. 231(13), 2016, 2417-2428. DOI: 0954406216636167
- [14] V Rajput, MM Goud, NM Suri. Numerical and experimental investigations to analyze the micro-hole drilling process in spark-assisted chemical engraving (SACE), *SN Appl Sci*, 2. <https://doi.org/10.1007/s42452-020-03311-y>
- [15] V Rajput, MM Goud, NM Suri. Finite element modelling for analyzing material removal rate in ECDM. *Journal of advanced manufacturing systems*, 2020. DOI: 10.1142/S0219686720500365
- [16] V Rajput V, MM Goud, NM Suri. Finite Element Modeling for Comparing the Machining Performance of Different Electrolytes in ECDM. *Arabian journal for science and technology*. DOI: 10.1007/s13369-020-05009-0